



# Synthesis and luminescent properties of two different $Y_2WO_6:Eu^{3+}$ phosphor phases



Jaime Llanos<sup>a,\*</sup>, Douglas Olivares<sup>a</sup>, Víctor Manríquez<sup>b</sup>, Darío Espinoza<sup>b</sup>, Ivan Brito<sup>c</sup>

<sup>a</sup>Departamento de Química, Universidad Católica del Norte, Avda. Angamos 0610, Antofagasta, Chile

<sup>b</sup>Departamento de Química, Universidad de Chile, Las Palmeras 3425, Santiago, Chile

<sup>c</sup>Departamento de Química, Universidad de Antofagasta, Campus Coloso, Antofagasta, Chile

## ARTICLE INFO

### Article history:

Received 24 September 2014

Received in revised form 5 December 2014

Accepted 16 December 2014

Available online 31 December 2014

### Keywords:

Inorganic materials

Optical materials

Photoluminescence

Aurivillius phases

## ABSTRACT

In this paper, two different  $Y_{2-x}Eu_xWO_6$  phases were synthesized. The monoclinic phase was prepared via a conventional solid-state reaction, whereas the orthorhombic phase was obtained via a facile, low-temperature combustion synthesis method. X-ray diffraction (XRD), scanning electron microscopy (SEM), differential scanning calorimetry (DSC), and photoluminescence (PL) spectroscopy were used to characterize the resulting phosphors. The XRD results indicate the orthorhombic phase crystallized isostructurally with the Aurivillius  $Bi_2WO_6$  phase, whereas the other polymorph crystallized isostructurally with  $Yb_2WO_6$  in the monoclinic system. The SEM studies revealed both phases had a strong tendency to form agglomerates averaging nanometers in size. The photoluminescence emission spectra confirmed all of the samples were efficiently excited by near UV light and were dominated by the electric dipole transition  $^5D_0 \rightarrow ^7F_2$ . The orthorhombic  $Y_{2-x}Eu_xWO_6$  excitation spectrum possessed a broad band across the entire UV region (220–400 nm); therefore,  $Y_{1.86}Eu_{0.14}WO_6$  could be considered an efficient spectral converter material for use in dye-sensitized solar cells.

© 2014 Elsevier B.V. All rights reserved.

## 1. Introduction

The chemistry of rare-earth elements plays an important role for both developing new solid-state lighting devices (SSLs) and improving solar cells. The main rare-earth compound applications in these areas have focused on the development of luminescent materials or energy converters, also known as inorganic phosphors [1–4].

An inorganic phosphor typically consists of an inert host material, normally an oxide, nitride, fluoride, sulfide, or oxysulfide, doped with a small concentration of an activator ion, usually a rare-earth (4f) cation. Although the choice of activator ions and host matrix depends on the specific phosphor application, the crystal chemistry of the matrix restricts the choices available. In this sense, the ionic radius of the activator ion must be similar to that of the host cation for an appropriate substitution upon doping [5–7]. Activator ions may be classified into two broad categories. For the first, the energy levels of the dopant ions involved during emission interact weakly with the host lattice.  $Ln^{3+}$  ions are typical examples of this class of activator, and the optical transitions only involve the 4f orbitals. For the second type of activator, s ( $Pb^{2+}$  or

$Sb^{3+}$ ) or d ( $Mn^{2+}$  or  $Eu^{2+}$ ) electrons are involved in the transition [8,9]. According to Jüstel et al., the strong electronic state coupling in the later yield lattice vibrations that lead to broad bands in the spectrum [1].

The host matrix is also important. The best host materials are divided into two types, optically inert and optically active; for optically inert hosts (oxides, silicates, phosphates, and fluorides), only the activator is involved during luminescence. Optically active anionic networks (tungstate and vanadate) are also involved in the luminescent process [10–12]. Therefore, rare-earth tungstates have attracted significant interest; alkali-metal rare-earth double tungstates,  $ARE(WO_4)_2$  ( $A = Li^+, Na^+, K^+, RE = Gd^{3+}, La^{3+},$  and  $Y^{3+}$ ), in particular have been widely investigated due to their optical properties and excellent thermal and chemical stabilities [13–16]. Tungstates with different stoichiometries, such as  $Ln_2WO_6$ , have been studied less probably due to the difficulty with obtaining pure phases [17]. Yttrium tungstate with a formula of  $Y_2WO_6$  is known to exhibit different crystallographic forms, monoclinic, tetragonal, etc., via the solid-state reaction at high temperature [18–21].

This paper is part of our continuing study on the synthesis, characterization, and luminescent properties of inorganic phosphors containing rare-earth cations [22–26]. In this report, we focused on the synthesis, characterization, and optical properties

\* Corresponding author. Tel.: +56 55 2 355624.

E-mail address: [jjlanos@ucn.cl](mailto:jjlanos@ucn.cl) (J. Llanos).

of two different phases for the inorganic phosphor  $Y_2WO_6$  doped with  $Eu^{3+}$ . The monoclinic form was prepared via a typical solid-state reaction, whereas the LT-phase was prepared via a low-temperature combustion synthesis [27,28]. The LT-phase exhibited broad absorption bands in the region from 250 to 390 nm, and emitted intense red visible light. These traits led us to propose  $LT-Y_2WO_6:Eu^{3+}$  as a potential spectral converter for dye-sensitized solar cells (DSSCs). The dopant ion concentration was also optimized.

## 2. Experimental

### 2.1. Synthesis

The monoclinic phase of  $Y_2WO_6:Eu^{3+}$  was prepared via a solid-state reaction at high temperature [27]. All phosphors were synthesized from a thoroughly ground mixture of the corresponding oxides,  $Y_2O_3$ ,  $Eu_2O_3$ , and  $WO_3$ , in stoichiometric proportions. The mixtures were placed in an alumina boat and heated to 973 K for 10 h before cooling to below 400 K. The sample was removed from the crucible, ground into a powder, and reheated for 10 h at 1273 K. The procedure was repeated, and the sample was finally heated to 1373 K for another 10 h. All of these synthetic processes were performed under an air atmosphere.

Powder X-ray diffraction (PXRD) data were collected using a Bruker D8 Advance diffractometer fitted with a graphite monochromator with  $Cu K\alpha$  radiation ( $\lambda = 1.54057 \text{ \AA}$ ) across the range from  $10 \leq 2\theta \leq 60$  to determine the phase purity. The experimental powder pattern for the doped and un-doped samples were almost in perfect agreement with those reported in the ICDS database and by Qin et al. and corresponded to the monoclinic phase of  $Y_2WO_6$  [28,29].

In contrast, the orthorhombic LT-phase for  $Y_2WO_6:Eu^{3+}$  was prepared via a facile low-temperature combustion synthesis. Based on the stoichiometric formula,  $Y_2O_3$  and  $Eu_2O_3$ , were dissolved in 10 ml of  $HNO_3$  ( $2 \text{ mol dm}^{-3}$ ) under vigorous agitation at 353 K. The solution pH was adjusted to between 1 and 2. When the oxides dissolved completely, the solution pH was adjusted to  $pH \approx 7$ . Meanwhile, 2.19 mmol of  $WO_3$  (Aldrich 99.995% pure) was dissolved in 7 ml of  $NaOH$  ( $5 \text{ mol dm}^{-3}$ ) in another beaker with vigorous stirring at 353 K. The resultant  $NaWO_4$  was dissolved in 5 ml of deionized water and mixed with 5 mmol of glycine. Both solutions were mixed to obtain a precursor suspension, which was concentrated in a beaker on a hot plate at 473 K with stirring. Reaching the critical temperature generated a small explosion accompanied by a large production of gases, which yielded a black product. Finally, the hot plate was turned off, and the sample was allowed to cool to room temperature. The product was ground in an agate mortar and annealed for 3 h at 673 K in a furnace. An optical inspection indicated the product was a homogeneous white powder. The experimental powder patterns agreed well with those reported in the literature [29].

### 2.2. Characterization

The phase purities were determined via an X-ray powder diffraction analysis (vide supra). The nanocrystalline  $Y_{2-x}Eu_xWO_6$  phosphor surface morphologies were determined via scanning electron microscopy (SEM, Jeol, JSM-6360LV). The thermal stability of the samples (10.468 mg) was analyzed using a Netzsch STA 449 F3 Jupiter apparatus with a heating rate of 10 K/min. The photoluminescence (PL) spectra (emission and excitation) were measured using a JASCO FP-6500 spectrofluorometer. All of the spectra were collected at room temperature. The sample quantities were identical across all experiments so the photoluminescence intensities could be compared.

## 3. Results and discussion

The monoclinic phase: 10 compositions were synthesized for the  $Y_{2-x}Eu_xWO_6$  system ( $x = 0.00; 0.02, 0.04, 0.06, 0.08, 0.10, 0.12, 0.14, 0.16, 0.18, \text{ and } 0.20$ ). The powder X-ray diffraction patterns for these compounds indicate all of the samples crystallized isostructurally with a monoclinic  $Y_2WO_6$  structure with a  $P2_1/c$  space group (No. 13). The powder diffraction patterns for the monoclinic  $Y_{2-x}Eu_xWO_6$  samples are shown in Fig. 1.

The Scherrer equation allows the crystallite size to be estimated. The Scherrer equation,  $D = 0.90\lambda/\beta\cos\theta$ , predicts the crystallite thickness for crystals smaller than 1000 Å because small angular differences are associated with large spatial distances (inverse space), so the diffraction peak broadening is expected to reflect the crystal size. In this equation,  $D$  is the average grain size,  $\lambda$  is the radiation wavelength used for the diffraction experiments,

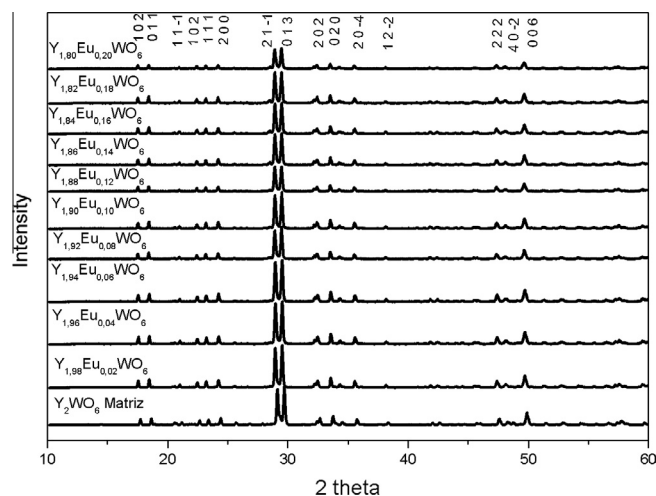


Fig. 1. XRD patterns of the monoclinic  $Y_2WO_6$  doped with different concentration of  $Eu^{3+}$ .

$\theta$  is the diffraction angle, and  $\beta$  is the full-width at half maximum (FWHM) for the observed peaks [30,31]. The strongest diffraction peak (013) was used to calculate the sample grain size. Our results indicate the crystallite sizes for monoclinic  $Y_{2-x}Eu_xWO_6$  ranged from 60 to 85 nm.

The crystallite morphology for monoclinic  $Y_{2-x}Eu_xWO_6$  was inspected via scanning electron microscopy (SEM). This study revealed the samples were spherical with a strong tendency to form aggregates as shown in Fig. 2.

The excitation spectrum for monoclinic  $Y_{2-x}Eu_xWO_6$  (shown in Fig. 3) exhibited a broad C–T band centered at 300 nm along with sharp  ${}^7F_0 \rightarrow {}^5L_6$  (395 nm) and  ${}^7F_0 \rightarrow {}^5D_2$  (465 nm) transitions. The C–T band intensity is much larger than the  $f \rightarrow f$  transitions. The broad, intense band consisted of overlaying  $O^{2-}-Eu^{3+}$  and  $O^{2-}-W^{6+}$  charge transfer bands.

The emission spectra for the monoclinic samples were dominated by the red peak due to the electric dipole transition in  $Y_{2-x}Eu_xWO_6$  at a wavelength of 300 nm, and an intense peak occurred at 611 nm. All of the spectra exhibited similar features, and the characteristic emission originated from the transition between the  ${}^5D_0$  excited state to the  ${}^7F_j$  ground state ( $j = 0, 1, 2, 3$  and 4) for the  $4f^6$  configuration of  $Eu^{3+}$ . The optimal  $Eu^{3+}$  doping concentration in the host was  $x = 0.14$  as shown in Fig. 4. The PL

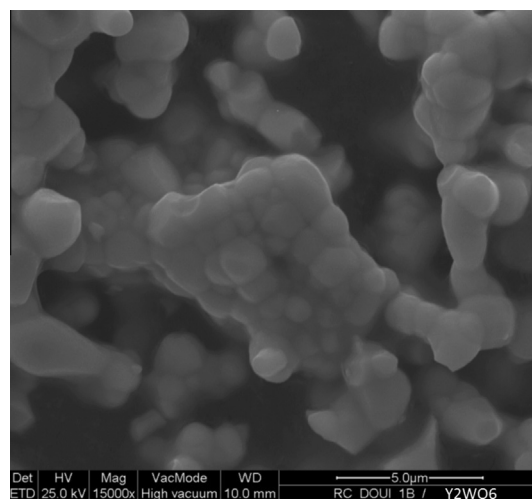


Fig. 2. SEM micrograph of  $Y_{1.86}Eu_{0.14}WO_6$  prepared by solid-state reaction.

Download English Version:

<https://daneshyari.com/en/article/7999578>

Download Persian Version:

<https://daneshyari.com/article/7999578>

[Daneshyari.com](https://daneshyari.com)